



Will calcium carbonate really scale in seawater reverse osmosis?

Tarek Waly^{a,b}, Saleh Saleh^a, Maria D. Kennedy^{a*}, Geert Jan Witkamp^c, Gary Amy^{a,b}, Jan C. Schippers^a

^aUNESCO-IHE, Institute for Water Education, Department of Urban Water and Sanitation, Westvest 7, 2611 AX Delft, The Netherlands
Tel: +31 15 2151715; email: m.kennedy@unesco-ihe.org

^bFaculty of Civil Engineering and Geoscience, Delft University of Technology, Stevinweg 1, Delft, The Netherlands

^cProcess and Energy Laboratory, Delft University of Technology, Leeghwaterstraat 44, Delft, The Netherlands

Received 14 October 2008; Accepted 8 March 2009

ABSTRACT

The elimination of antiscalant chemicals in SWRO plants will result in a more environmentally friendly, sustainable and cheaper process. Practically, this can be achieved by determining the real scaling limits of calcium carbonate in SWRO. In supersaturated solutions the period of metastability before the start of crystal growth is commonly indicated as induction time (t_{ind}). Induction time longer than the average retention time of concentrate in a single-stage SWRO suggests that scaling will probably not occur. This research project aims to determine the induction times as a function of the saturation index and ionic strength for synthetic seawater. The experimental procedure utilized in this research is a sensitive and stable pH meter with accuracy of 0.01 pH units. The pH meter used was able to detect precipitation as low as 0.3 mg/l of CaCO_3 . Induction time experiments were performed with synthetic concentrates with low and high ionic strength. The synthetic high ionic strength solution had the same ionic strength, Ca^{2+} and HCO_3^- concentrations as the SWRO concentrate at a recovery of 30% and utilizing water from the Gulf of Oman. The lower ionic strength solution comprise the same Ca^{2+} and HCO_3^- concentrations as of the high ionic solution but with lower NaCl content. Results showed a good correlation between the logarithm of the induction time and saturation index. The pH of SWRO concentrate with (30% recovery) is expected to be in the range of 8.25–8.3. Experimental results showed an induction time of almost 30 min using synthetic concentrate which is ca. 10–15 times longer than the average retention time of concentrate in a single-stage SWRO (2–3 min). These results need to be verified with real SWRO concentrate.

Keywords: Induction time; Membrane; Calcite; Scaling; Antiscalant; Acid

1. Introduction

SWRO plants use acid and/or antiscalant to prevent the precipitation of calcium carbonate and calcium sulfate. The application of these chemicals not only increases the

total plant cost, but increases the burden to the environment as well. Furthermore, some antiscalants or contaminated acid may promote biofouling in SWRO plants. The use of one or both chemicals is based on theoretical calculations of the solubility of these compounds. Commonly, the ASTM approach is used to calculate the solubility of CaCO_3 .

*Corresponding author.

From the scientific literature [1–3], laboratory experiments with low salinity water indicated that precipitation of CaCO₃ does not occur unless calcite solubility is exceeded 100 times. Evidence from practice also suggests that eliminating/minimize antiscalant and acid addition in SWRO plants is achievable, as a limited number of full scale plants use acid alone while others work without acid or antiscalant and simply flush the SWRO membrane once a week with acid.

SWRO plants commonly use acid and/or antiscalant to prevent the precipitation of calcium carbonate. The application of these chemicals not only increases the total plant cost, but increases the burden to the environment as well. Furthermore, some antiscalants or contaminated acid may promote biofouling in SWRO plants. The use of one or both chemicals is based on theoretical calculations of the solubility of these compounds [4]. In the Middle East, seawater TDS normally ranges between 35,000 mg/L (Mediterranean) and 45,000 mg/L (parts of the Gulf and Red Sea). Average values as shown in Table 1 are commonly found depending on the extraction method (open intake or beach well) and the intake extraction depth.

Different methods are used to assess the calcium carbonate scaling potentiality in seawater. The methods commonly used are the Stiff & Davis saturation index (S&DSI), saturation index (SI) and the Saturation Ratio (S_r). The former can be expressed as:

$$S\&DSI = pH_c - pH_s \tag{1}$$

where

$$pH_s = pCa + pAlk + k \tag{2}$$

and *k* is a factor related to the concentrate ionic strength

Table 1
Gulf of Oman water constitute (Source: MEDRC database)

Ions		Inlet (mg/L)	Inlet (mmol/L)
pH		8.09	
Alkalinity	as CaCO ₃	120	
Magnesium	Mg ⁺²	1,355.6	55.8
Sodium	Na ⁺¹	12,244.7	532.6
Potassium	K ⁺²	434	11.1
Carbonate	CO ₃ ⁻²	23.16	0.4
Sulphate	SO ₄ ⁻²	2,772	28.9
Chlorides	CL ⁻¹	21,535	607.4
Calcium	Ca	474	11.9
Ammonium	NH ₄	0.039	0.0
Phosphate	PO ₄	0.245	0.0
Silica	SiO ₂ ⁻²	0.13	0.00
TDS		38,839	
Ionic strength			0.79

and temperature. In this approach the effect of temperature and salinity (ionic strength) on dissociation and solubility is corrected by this factor.

The ionic strength limit of the concentrate ranges between 0–2.0 M and temperatures from 0 to 50°C, making it a very useful tool for calcium carbonate scaling determination in seawater reverse osmosis plants. Following the same concept, however, it is more accurate to make use of activities of the ions. The activities depend on temperature and interactions between the ions. Saturation ratio and saturation index can be defined through the following equations.

- For salt



$$S_r = \left(\frac{\gamma_+ [Ca^{2+}] \cdot \gamma_- [CO_3^{2-}]}{K_{sp}} \right)^{\frac{1}{2}} \tag{4}$$

while

$$SI = \log \left(\frac{\gamma_+ [Ca^{2+}] \cdot \gamma_- [CO_3^{2-}]}{K_{sp}} \right) \tag{5}$$

where γ_+ and γ_- are the activity coefficient for Ca²⁺ and CO₃⁻² respectively. Different methods, e.g., Debye–Huckel and Bromly and Pitzer, are commonly used for activity coefficient calculations [5]. The methods are adopted based on feed water ionic strength and constitute. The activity calculations can be done manually or with the help of chemical equilibrium software programs (e.g., Phreeqc; Minteq and Aquachem) that incorporate these methods in their calculations.

Values of *S_r* and *SI* greater than 1 and 0, respectively, mean that calcium carbonate will precipitate, while values less than 1 and 0 mean that the solution is under saturated with respect to this specific salt.

Although it is commonly assumed that supersaturation will result in instantaneous precipitation, many researchers have claimed that this, to a great extent, is not true. These researchers tried to modify the existing indices to predict correctly when CaCO₃ will precipitate. The main approach was to consider the effect of ionic strength and temperature on calcite solubility [6–10]. Others claimed that other forms of CaCO₃ are the most critical and hence, their solubilities must be taken in the saturation calculations instead of calcite [1,11,12].

Induction time is defined as the time lag between nucleation and subsequent growth. In practice the concept of *induction time* is frequently used to describe nucleation. Induction time is defined as the time elapsed between the

creation of supersaturation and the first appearance of a new phase, ideally nuclei with the critical cluster size dimensions [13]. Induction time may be measured by following the change in concentration of one of the crystal ions, pH, conductivity meter or turbidity meter over time [5].

Experimentally, it is very difficult to determine the formation of the first nuclei, and consequently, a part of the induction time may also include growth to a detectable size. For the purposes of this research it is assumed that the nucleation time is much greater than the time required for growth of crystal nuclei to a detectable size. Thus, induction time can be assumed to be inversely proportional to the rate of nucleation, $t_{\text{ind}} \propto J^{-1}$ [13]:

$$t_{\text{ind}} = J^{-1} \quad (6)$$

where the steady-state nucleation rate can be expressed in

$$J_s = \Omega \exp \left[\frac{\beta V_m^2 \gamma^s \cdot f(\theta)}{v^2 (kT)^3 (\ln S_r^2)^2} \right] \quad (7)$$

The value of $f(\theta)$ determines the nucleation mechanism. Homogeneous nucleation is recognized by $f(\theta) = 1$ while for heterogeneous nucleation $f(\theta) < 1$. Values as low as 0.01 were reported for $f(\theta)$ [13].

Based on Eqs. (6) and (7),

$$\log t_{\text{ind}} = \frac{B}{T^3 (\log S_r^2)^2} - A \quad (8)$$

where

$$B = \frac{\beta V_m^2 \gamma^s f(\theta)}{v^2 (2.3k)^3} \quad (9)$$

and

$$A = \log \Omega \quad (10)$$

For spherical shape crystals $\beta = \frac{16\pi}{3}$. This is a factor relating the volume of the crystal with its area [13].

2. Materials and methods

Methods used to measure induction period are various and diverse. The most common methods used are calcium specific electrode, conductivity meter, pH meter, ICP or AAS, (laser) turbidity meter and UV absorbance.

Generally, the faster the method's ability to detect the first formed crystals, the more accurate induction time can be determined.

In this research induction time was monitored using a highly sensitive and stable pH meter with an accuracy of 0.01 pH units. The pH drop was monitored over a 24 h period, and induction time was defined as the point when the pH decreased by at least 0.03 pH units. This decrease is equivalent to 0.3 mg/L of precipitated CaCO_3 . The pH meter was attached to a double walled glass reactor with tight air sealing and a mechanical mixer. The mixer shaft was equipped with two paddles to insure proper and homogeneous mixing for the reagents. Higher mixing speed was used during the addition of the reagent solutions to prevent zones of high local saturation. The pH meter was linked to computer where pH measuring intervals were set at 1 min.

Experimental work was performed with synthetic concentrates with total dissolved salt concentrations equal to 2165 mg/l or 55,215 mg/l. The used water type contained: HCO_3^- (209 mg/l) and Ca^{2+} (667 mg/l) while NaCl was added to reach different ionic strengths. Two types, as shown in Table 2, have HCO_3^- and Ca^{2+} concentrations equivalent to that in SWRO concentrates of 30% recovery for feed water of nearly 39,000 mg/l of total dissolved solids. The effect of ionic strength on induction period was tested by increasing the NaCl content in the second batch.

The synthetic water pH was varied as shown in Table 2 in steps of 0.2 pH units using 0.1 molar NaOH. Varying the pH results in a change in the saturation index of the low ionic strength solution from up 1.2 till 2.11 and from 0.13 till nearly 0.93 for the higher ionic strength one. The relation between the pH; saturation index and induction time was determined for each test independently.

Experimental solutions were made utilizing pro-analytical grade salts as shown in Table 3. The salts were dissolved in milli Q water with conductivity less than 4 $\mu\text{S}/\text{cm}$.

Table 2

Experimental feed water pH and corresponding saturation index

Low Ionic strength = 0.054 mole/L		High ionic strength = 0.96 mole/L	
Feed pH	Feed SI	Feed pH	Feed SI
7.84	1.2	8.07	0.13
8.02	1.38	8.27	0.33
8.27	1.63	8.42	0.48
8.4	1.76	8.69	0.75
8.57	1.93	8.88	0.93
8.75	2.11		

Table 3
Test reagent

Reagent	Form
NaCl	Salt
CaCl ₂ ·2H ₂ O	Salt
NaHCO ₃	Salt

Table 4
Experimental synthetic water composition

Ions	Low ionic strength = 0.054		High ionic strength = 0.96	
	mg/l	mmol/l	mg/l	mmol/l
Temperature °C	25		25	
Calcium Ca ²⁺	677.1	16.9	677.1	16.9
Sodium Na ⁺	78.9	3.4	20,936	910.7
Bicarbonate HCO ₃ ⁻	209.1	3.4	209.1	3.4
Chloride Cl ⁻	1,200.3	33.9	33,392.9	941.9
TDS	2,165.5		55,215.2	
Ionic strength	0.054		0.96	

The experimental work was done on two different levels of ionic strength as shown in Table 4 to measure its effect on induction period. The results were fit to Eq. (8) and compared with previous researchers' results.

The calculation method for SI and S_r follows the following procedure:

- For salt



$$SI = \log \left(\frac{[X] \cdot [Y]}{K_{sp}} \right) = \log([X] \cdot [Y]) - \log(K_{sp}) \quad (12)$$

$$= \log(IAP) - \log(K_{sp})$$

while

$$S_r = \left(\frac{[X] \cdot [Y]}{K_{sp}} \right)^{\frac{1}{v_c + v_a}} \quad (13)$$

$$\begin{aligned} \therefore \log S_r &= \log \left(\frac{[X] \cdot [Y]}{K_{sp}} \right)^{\frac{1}{v_c + v_a}} = \frac{1}{v_c + v_a} \log \left(\frac{[X] \cdot [Y]}{K_{sp}} \right) \\ &= \frac{1}{v_c + v_a} x SI \end{aligned} \quad (14)$$

$$\therefore SI = (v_c + v_a) \log S_r \quad (15)$$

- In our specific case of CaCO₃:

$$\therefore SI = 2 \log S_r \quad (16)$$

- For the relation between S&DSI and SI:

$$S\&DSI = pH_c - pH_s \quad (17)$$

where

$$pH_s = pCa + pAlk + k \quad (18)$$

and

$$k = pK_{a2} - pK_{sp} \quad (19)$$

$$S\&DSI = pH - pH_s = pH - pCa - pAlk - pK_{a2} + pK_{sp} \quad (20)$$

$$\therefore Alk = HCO_3^- \quad (21)$$

and

$$K_{a2}[HCO_3^-] = [CO_3^{2-}][H^+] \quad (22)$$

$$\therefore pK_{a2} + p[HCO_3^-] = p[CO_3^{2-}] + p[H^+] \quad (23)$$

$$\therefore -p[CO_3^{2-}] = pH - pK_{a2} - p[HCO_3^-] \quad (24)$$

By substituting in Eq. (18)

$$S\&DSI = -pCO_3^{2-} - pCa^{2+} + pK_{sp} = \log[CO_3^{2-}] + \log[Ca^{2+}] - \log K_{sp} \quad (25)$$

$$\therefore S\&SDI = \log[IAP] - \log K_{sp} = SI \quad (26)$$

3. Results and discussion

The relation between pH and time was investigated for each feed pH in duplicate over a period of 1000 min. In Fig. 1 the pH vs. time is presented for feed water with ionic strength of 0.96 at 25°C and initial S&DSI of 0.93. Fig. 1 can be subdivided into three stages in the precipitation process. In spite of the stability indicated in the first period (up to 25 min), a rapid decrease in pH with time

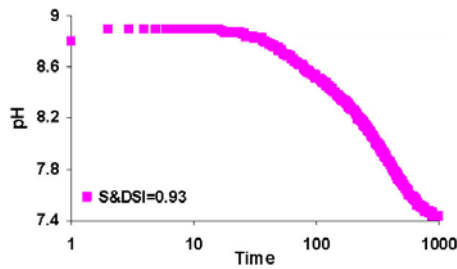


Fig. 1. Time (min) vs pH for high ionic strength water at temperature 25°C and initial S&DSI = 0.93.

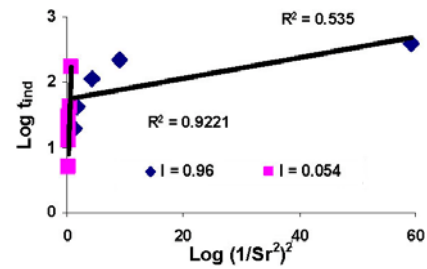


Fig. 3. Log t_{ind} (min) vs. $\log (1/Sr^2)$ for high ionic strength water.

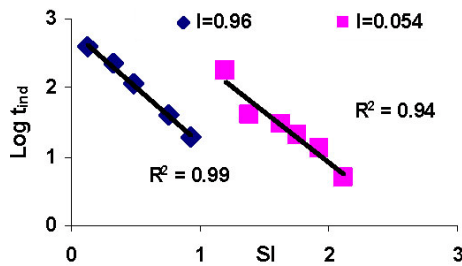


Fig. 2. Log t_{ind} (min) vs. SI for low and high ionic strength water at 25°C.

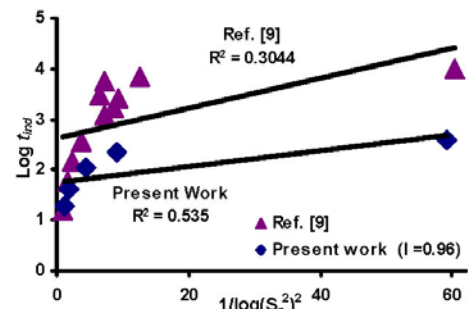


Fig. 4a. Comparison relationship between $\log t_{ind}$ (min) vs. $\log (1/Sr^2)$ with literature sources [9] with experimental results.

Table 5

Feed water pH and corresponding saturation index in relation with induction time

Low ionic strength ($I=0.054$)			High ionic strength ($I=0.96$)		
Feed pH	Feed SI	t_{ind} (min)	Feed pH	Feed SI	t_{ind} (min)
7.84	1.2	173 ± 18	8.07	0.13	398 ± 48
8.02	1.38	41 ± 3	8.27	0.33	223 ± 15
8.27	1.63	30 ± 7	8.42	0.48	114 ± 5
8.4	1.76	20 ± 2	8.69	0.75	41 ± 7
8.57	1.93	13 ± 2	8.88	0.93	23 ± 8
8.75	2.11	5 ± 2			

was experienced as the critical nuclei size is surpassed (up to 900 min) in the second. phase. The last stage is recognized by a slower decrease in pH with time where solution saturation, representing the driving force for nucleation, becomes slower.

The relation relating the SI vs. t_{ind} shown in Fig. 2 utilizing the results in Table 5 revealed a good fit with a correlation coefficient (R^2) from 94–99%. The induction period in low ionic strength ($I = 0.054$) water ranges from 5 ± 2 min to 173 ± 12 min for SI from 2.11 to 1.2, respectively. In the case of high ionic strength water, the induction period ranged between 23 ± 8 and 398 ± 48 min for SI ranges between 0.93 and 0.13, respectively. An induction time of zero (spontaneous precipitation) was not found in our experimental range.

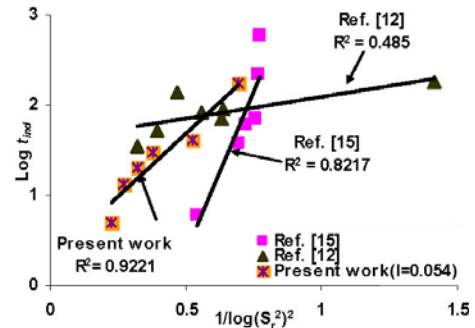


Fig. 4b. Comparison relationship between $\log t_{ind}$ (min) vs. $\log (1/Sr^2)$ with literature sources [12,15] with experimental results.

In real SWRO working on 30% recovery and with the same Ca^{2+} and HCO_3^- constituents used, the concentrate has SI of nearly 0.33. In this specific range, results show an induction time of nearly 223 min. This obtained induction value is nearly 100 times greater than the average retention time of the concentrate in SWRO plant (2–3 min) [14]. This suggests that concentrates with the same Ca^{2+} and HCO_3^- concentration might not scale inside a SWRO plant.

Experimental results shown in Fig. 3 revealed a poor correlation between $\log t_{ind}$ and $1/(\log S_r^2)$ at lower S_r levels with R^2 of 0.54. This was not the case for high S_r values where the relation demonstrates a good fit with R^2 factor of nearly 0.92.

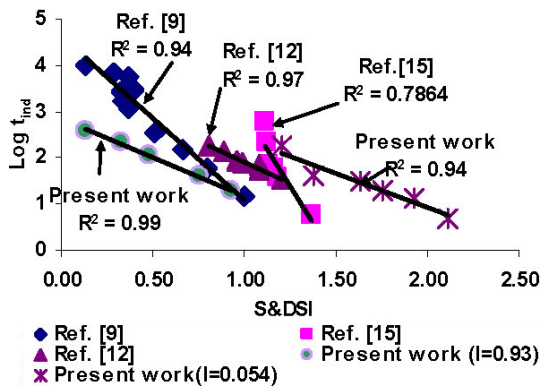


Fig. 5. Comparison relationship between $\log t_{ind}$ (min) vs. SI for three different literature sources [9,12,15] with experimental results.

Literature data were used for comparison of results using $\log t_{ind}$ vs. $1/(\log S_r^2)^2$ and $\log t_{ind}$ vs. SI [9,12,15]. These studies cover different ionic strengths with a minimum of 0.3 [9] and a maximum of 1.0 [12]. Similar to what was found in Fig. 3, the relation shown in Figs. 4a and 4b reveal a poor correlation between $\log t_{ind}$ vs. $1/(\log S_r^2)^2$ except for Koutsoukoas and Kontoyannis [15] and the present work ($I = 0.054$) where both used high S_r in their experimental work. Adopting the $\log t_{ind}$ vs. SI in Fig. 5 results in a considerable improvement in the R^2 . The best improvement was for Butt et al. [9] where R^2 increased from 0.3 to 0.94, followed by Hannachi et al. [12] from 0.485 to 0.97 while in Koutsoukoas and Kontoyannis [15] R^2 decreased slightly from 0.82 to 0.79. The results represented in Fig. 5 show that a good fit was found for both high and low SI values.

4. Conclusions

1. Duplicate measurements show that a sensitive and stable pH meter was capable of measuring the induction time for supersaturated synthetic solutions with accuracy of just 0.3 mg/l of precipitated $CaCO_3$.

2. The relation between the logarithm of the inducing time vs. SI gave a better fit than the commonly reported relation $\log t_{ind}$ vs. $1/(\log S_r^2)^2$.

3. The measured induction time in high salinity water representing concentrate of a SWRO plant operating at 30% recovery having a pH of 8.3 was about 200 min. This suggests scaling will not occur in a SWRO since the residence time is just a couple of minutes.

4. Further research with water having a composition closer to the water in the Gulf will be conducted to know whether there is a general relation between induction time and the probability of scaling of $CaCO_3$ in full-scale seawater reverse osmosis plants.

5. Symbols

- A — Function of pre-exponential factor, $s^{-1}m^{-3}$
 - A^* — Debye–Huckel constant, $L^{2/3}mol^{-1/2}$
 - a_c — Activity
 - A_f — Free area for precipitation at given particle size, m^2
 - Alk — Alkalinity of solution, mole/L
 - B — Constant expressed in Eq. (8), $L^{3/2}mol^{-1/2}nm^{-1}$
 - $f(\theta)$ — Factor differentiating heterogeneous and homogeneous nucleation
 - I — Ionic strength, mol/L
 - IAP — ionic activity product, mol^2/L^2
 - J — Nucleation rate, nuclei/min/ cm^3
 - J_s — Steady-state nucleation rate, nuclei/min/ cm^3
 - k — Boltzmann constant, J/K
 - K_{sp} — Solubility product, $mole^2/L^2$
 - K_{a2} — Second acidity constant, mole/L
 - P — Pressure, psi
 - pH_c — Concentrate pH
 - pH_s — Equilibrium pH
 - S_r — Supersaturation ratio
 - SI — Supersaturation Index
 - T — Absolute temperature, K
 - t_{ind} — Induction time in minutes unless mentioned otherwise, min
 - v — Number of ions into which a molecule dissociate
 - v_a — Number of anions into which a molecule dissociate
 - v_c — Number of cations into which a molecule dissociate
 - V_m — Molecular volume, $cm^3/mole$
- Greek*
- β — Geometric factor
 - γ_+ — Cation activity coefficient
 - γ_- — Anion activity coefficient
 - γ^s — Surface energy, J/ m^2
 - Ω — Pre-exponential factor in the nucleation rate equation, $s^{-1}m^{-3}$

References

- [1] J. Gal, Y. Fovet and N. Gache, Water Res., 36 (2002) 764–773.
- [2] H. Elfil and H. Roques, Desalination, 137 (2001) 177–186.
- [3] F. Alimi, H. Elfil and A. Gadrib, Desalination, 157 (2003) 9–16.
- [4] M. Al-Shammiri and M. Al-Dawas, Desalination, 110 (1997) 37–48.
- [5] S. Boerlage, Scaling and particulate fouling in membrane filtration system, PhD Thesis, IHE, Delft, 2002.
- [6] R. Sheikholeslami, Desalination, 167 (2004) 247–256.
- [7] S.E. Ingle, Marine Chem., 3 (1975) 301–319.
- [8] L. Plummer and E. Busenberg, Geochimica et Cosmochimica Acta, 46 (1982) 1011–1040.
- [9] F.H. Butt, F. Rahman, and U. Baduruthamal, Desalination, 144 (1997) 51–64.

- [10] P. Zuddas and A. Mucci, *Geochimica et Cosmochimica Acta*, 58 (1994) 4353–4362.
- [11] H. Elfil and A. Hannachi, *AIChE J.*, 52 (2006) 3583–3591.
- [12] A. Hannachi, I. Naimi, R. Zinoubi and H. Elfil, in: *Proc. IDA World Congress, Maspalomas, Gran Canaria, 2007*.
- [13] O. Sohnle and J. Garsida, *Precipitation Basis Principles and Industrial Applications*, Butterworth-Heinemann, Oxford, 1992.
- [14] D. Hasson, A. Dark, C. Komlos, Q. Yang and R. Semiat, *Desalination*, 204 (2007) 132–144.
- [15] P. Koutsoukoas and C. Kontoyannis, *J. Chem. Soc., Faraday Trans.*, 80 (1984) 1181–1192.